AINTEGUMENTA and AINTEGUMENTA-LIKE6/PLETHORA3 Induce *LEAFY* Expression in Response to Auxin to Promote the Onset of Flower Formation in Arabidopsis[1][OPEN]

Nobutoshi Yamaguchi[2], Cheol Woong Jeong, Staci Nole-Wilson, Beth A. Krizek, and Doris Wagner*

Department of Biology, University of Pennsylvania, Philadelphia, Pennsylvania 19104–6018 (N.Y., C.W.J., D.W.); and Department of Biological Sciences, University of South Carolina, Columbia, South Carolina 29208 (S.N.-W., B.A.K.)

ORCID IDs: 0000-0003-0002-7652 (C.W.J.); 0000-0001-5821-0180 (B.K.).

Proper timing of the onset to flower formation is critical for reproductive success. Monocarpic plants like Arabidopsis (*Arabidopsis thaliana*) switch from production of branches in the axils of leaves to that of flowers once in their lifecycle, during the meristem identity transition. The plant-specific transcription factor LEAFY (LFY) is necessary and sufficient for this transition. Previously, we reported that the plant hormone auxin induces *LFY* expression through AUXIN RESPONSE FACTOR5/MONOPTEROS (ARF5/MP). It is not known whether MP is solely responsible for auxin-directed transcriptional activation of *LFY*. Here, we show that two transcription factors belonging to the AINTEGUMENTA-LIKE/PLETHORA family, AINTEGUMENTA (ANT) and AINTEGUMENTA-LIKE6/PLETHORA3 (AIL6/PLT3), act in parallel with MP to upregulate *LFY* in response to auxin. *ant ail6* mutants display a delay in the meristem identity transition and in *LFY* induction. ANT and AIL6/PLT3 are expressed prior to *LFY* and bind to the *LFY* promoter to control *LFY* mRNA accumulation. Genetic and promoter/reporter studies suggest that ANT/AIL6 act in parallel with MP to promote *LFY* induction in response to auxin sensing. Our study highlights the importance of two separate auxin-controlled pathways in the meristem identity transition.

The switch to flower formation is a critical step in the plant life cycle and is accompanied by a transition from biomass and resource production to resource allocation to the next generation (Araki, 2001; Poethig, 2003; Bäurle and Dean, 2006; Blázquez et al., 2006). After embryonic development, the stem-cell pool containing shoot apical meristem gives rise to new lateral organs such as leaves or flowers (Steeves and Sussex, 1989). The switch to flower formation is biphasic in Arabidopsis (*Arabidopsis thaliana*) and other monocarpic plants (Hempel et al., 1997; Ratcliffe et al., 1999; Poethig, 2003; Yamaguchi et al., 2014). First comes the transition from the vegetative phase, in which rosette leaves are produced, to the prefloral inflorescence phase (Yamaguchi et al., 2014). In this initial phase of inflorescence development, primordia at the flanks of the shoot apical meristem form cauline leaves that subtend secondary inflorescence branches (Ratcliffe et al., 1999). Once plants are fully reproductively competent, primordia instead give rise to the reproductive structures, the flowers (Hempel et al., 1997; Ratcliffe et al., 1999; Poethig, 2003; Yamaguchi et al., 2014). The transition to the floral inflorescence phase is frequently referred to as the meristem identity transition.

The plant-specific transcription factor LEAFY (LFY) is considered a master regulator of the switch from the prefloral to the floral inflorescence phase. Loss of LFY function dramatically delays formation of the first flower, while elevated levels of LFY trigger a precocious onset of flower formation (Weigel et al., 1992; Weigel and Nilsson, 1995). Moreover, spatiotemporal *LFY* accumulation is a critical determinant of when and where flowers form (Blázquez et al., 1997; Yoon and Baum, 2004). Known cues that direct *LFY* upregulation are photoperiod, plant age, and hormones. For example, the MADS-box transcription factor pair SUPPRESSOR OF OVEREXPRESSION OF CO1 (SOC1) and AGAMOUS-LIKE24 (AGL24) upregulate *LFY* expression in response to inductive long day photoperiods (Lee et al., 2008; Liu et al., 2008). The micro-RNA regulated SBP-box transcription factor

[1] This work was supported by the U.S. National Science Foundation (grant no. IOS 1257111 to D.W. and IOS grant no. 0922367), the Department of Education (grant no. 98ER20312 to B.K.), and a Japan Society for the Promotion of Science Postdoctoral Fellowship for Research Abroad to N.Y.

[2] Present address: Graduate School of Biological Science, Nara Institute of Science and Technology, Nara 630–0192, Japan.

* Address correspondence to wagnerdo@sas.upenn.edu.

The author responsible for distribution of materials integral to the findings presented in this article in accordance with the policy described in the Instructions for Authors (www.plantphysiol.org) is: Doris Wagner (wagnerdo@sas.upenn.edu).

N.Y. and D.W. conceived the study; S.N.-W. and B.A.K. generated and characterized genetic materials; C.W.J. generated GUS lines and performed expression analysis; N.Y., D.W., and B.A.K. wrote and edited the article.

[OPEN] Articles can be viewed without a subscription.

www.plantphysiol.org/cgi/doi/10.1104/pp.15.00969

SQUAMOSA PROMOTER BINDING PROTEIN-LIKE3 (SPL3), a component of the age-sensing pathway, also induces *LFY* expression (Yamaguchi et al., 2009). In noninductive (short day) growth conditions, the plant hormone gibberellin is important for upregulation of *LFY* expression; this response is thought to be mediated by GAMYB proteins (Blázquez and Weigel, 2000; Gocal et al., 2001). More recently, a second hormone, auxin, has been implicated in upregulation of *LFY* expression. The AUXIN RESPONSE FACTOR5/MONOPTEROS (ARF5/MP) directly induces *LFY* expression upon auxin sensing (Yamaguchi et al., 2013). Two evolutionarily conserved and functionally important cis regulatory modules have been described for the approximately 2.3-kilobase-long 5′ intergenic region upstream of *LFY* (Blázquez and Weigel, 2000; Yamaguchi et al., 2013). Thus far, important sequence specific binding proteins have been linked to only one of these, the proximal or "P" cis regulatory module. MP specifically binds to this region. No other cis regions or trans factors have as yet been implicated in auxin responsiveness of *LFY*.

The eight members of the AINTEGUMENTA-LIKE/PLETHORA (AIL/PLT) transcription factor family are key developmental regulators with partially overlapping roles in many aspects of plant development, including embryogenesis, stem cell specification, meristem maintenance, positioning of lateral organs in the root and stem, and organ growth (Horstman et al., 2014). In many instances, the roles of these transcription factors have been linked to hormones, particularly auxin (Horstman et al., 2014). Two AIL/PLT proteins, PLT1 and PLT2, function downstream of auxin in specification of the root stem cell niche and feed back to regulate expression of *PIN-FORMED* auxin efflux genes, stabilizing an auxin maximum in these cells (Aida et al., 2004; Blilou et al., 2005). AIL5/PLT5, AIL6/PLT3, and AIL7/PLT7 control the positioning of lateral root initiation downstream of ARF7 and ARF19 and regulate shoot phyllotaxy by promoting auxin biosynthesis in the shoot apical meristem (Prasad et al., 2011; Hofhuis et al., 2013; Pinon et al., 2013). ANT and AIL6 regulate many aspects of flower development, some of which have been linked to auxin as well (Krizek, 2011a, 2011b). For example, ANT and AIL6 promote flower primordia initiation downstream of MP (Yamaguchi et al., 2013). In floral organ growth, ANT acts downstream of the auxin inducible AUXIN REGULATED GENE INVOLVED IN ORGAN SIZE (ARGOS; Hu et al., 2003). Other roles of ANT and AIL6 in flower development, including floral organ initiation, identity specification, and gynoecium patterning, may also involve auxin (Krizek, 2009).

Here, we show that auxin-activated ANT and AIL6 are redundantly required for the proper timing of the onset of flower formation. ANT and AIL6 execute this role by binding to the *LFY* promoter to induce *LFY* expression in incipient primordia. We further demonstrate that these two AIL/PLT transcription factors act in parallel with MP to induce *LFY* expression. Our study identifies the regions of the *LFY* promoter and the transacting factors that mediate auxin responsiveness of the locus and highlights the importance of the hormonal auxin cue in *LFY* induction at the onset of flower formation.

RESULTS

MP and Four Conserved Auxin Response Elements Located in the P Region Are Not Solely Responsible for Auxin-Mediated *LFY* Activation

The characterized full-length *LFY* "promoter" (henceforth referred to as *pLFY*) consists of an approximately 2.3-kilobase-long 5′ intergenic region upstream of *LFY* (Blázquez et al., 1997). *pLFY* contains two evolutionarily conserved, functionally important regions, the distal or "D" region and the proximal or "P" region (Blázquez and Weigel, 2000; Yamaguchi et al., 2013). A minimal *LFY* promoter (*pGOF9*), which only contains the conserved D and P regions as well as the core promoter (approximately 800 base pairs in total), recapitulates most of the activity of *pLFY* (Blázquez and Weigel, 2000). Recently, the auxin responsive transcription factor MP was shown to directly induce *LFY* expression upon auxin sensing (Yamaguchi et al., 2013). MP binds in vivo to a single region of the endogenous *LFY* locus, the P region, and MP binding is dependent on four evolutionarily conserved core auxin response elements (AuxREs) in the P region (Yamaguchi et al., 2013). When we mutagenized all four AuxREs in the context of *pGOF9* driving a GFP-tagged version of the *LFY* cDNA, *LFY* expression was much reduced and the mutated minimal promoter *pGOF9* was essentially unresponsive to auxin (Yamaguchi et al., 2013). Auxin responsiveness in the context of the full-length *pLFY* has not been studied yet, but it is known that *pLFY* contains redundantly acting cis regions (Blázquez and Weigel, 2000).

To test whether the four AuxREs in the P region alone are responsible for auxin-mediated *LFY* activation by *pLFY*, we performed reporter analyses using full-length *pLFY* promoter. We assayed reporter activity in representative T2 plants. Synthetic auxin (2,4-dichlorophenoxyacetic acid [2,4-D]) application triggered an increase in *GUS* expression in the *pLFY::GUS* transgenic plants, as reported previously (Bai and Demason, 2008; Yamaguchi et al., 2013; Fig. 1, A and B). We also generated transgenic plants expressing a *pLFYAm*::*GUS* construct, in which all four AuxREs (TGTC) in the P region were converted to TGgC as previously described (Muller and Sheen, 2008; Yamaguchi et al., 2013). Surprisingly, *pLFYAm*::*GUS* was still responsive to auxin (Fig. 1B). An auxin-upregulated gene, MP (Lau et al., 2011), and endogenous *LFY* served as treatment controls (Yamaguchi et al., 2013; Supplemental Fig. S1). Because the same mutations in these AuxREs in the minimal *pGOF9* promoter abolished auxin responsiveness and because MP only binds to the P region of *pLFY* (Yamaguchi et al., 2013), these results suggest that MP is not solely responsible for auxin-mediated *LFY* activation

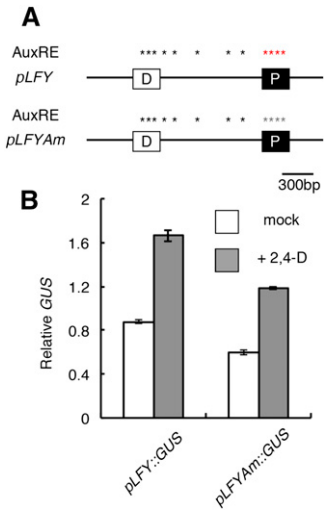

Figure 1. MP contributes to, but is not solely responsible for, auxin-mediated *LFY* activation. A, Diagram of *LFY* promoter with location of MP-bound cis elements (AuxREs). Boxes denote conserved regions of the *LFY* promoter. Asterisks, AuxREs; red asterisks, MP-bound core AuxREs; gray asterisks, mutated sites. B, *GUS* mRNA accumulation determined by qRT-PCR in reporter constructs driven by full-length upstream intergenic region (*pLFY*::*GUS*) and a version of *pLFY*::*GUS* in which the mutated four AuxREs in the P region were mutated (*pLFYAm*::*GUS*). RNA was isolated 3 h after application of mock or 2,4-D (10 μM) solution. Shown is the mean and SEM of *GUS* expression in representative transgenic plants normalized over that of *UBQ10* (*At4g05320*).

and that other transcription factor(s) likely act in parallel with MP to activate *LFY* in response to auxin via regions of the *LFY* promoter not present in *pGOF9*.

The Transcription Factors ANT and AIL6/PLT3 Promote Floral Meristem Identity Upstream of *LFY*

To identify additional trans factors that could mediate auxin responsiveness of *LFY*, we focused on the AIL/PLT transcription factor family (Horstman et al., 2014). Among these, ANT and AIL6/PLT3 play important roles in many aspects of flower development from flower primordium initiation to cell proliferation in incipient floral primordia, flower patterning, and elaboration of floral organ form (Elliott et al., 1996; Klucher et al., 1996; Krizek, 1999; Mizukami and Fischer, 2000; Krizek, 2009). Several of these pathways have links to auxin (Krizek, 2011a, 2011b). We hypothesized that ANT and AIL6 might regulate *LFY* downstream of auxin.

To test this hypothesis, we first compared the spatiotemporal accumulation of *LFY*, *ANT*, and *AIL6* at the times and in the tissues of interest. When grown in inductive photoperiod, the first flower appears in 15-d-old plants. On the basis of quantitative real-time PCR (qRT-PCR), *ANT* and *AIL6* transcripts start to accumulate in 5-d-old to 7-d-old wild-type seedlings, prior to *LFY* upregulation (Fig. 2A). Similar data were obtained when querying public transcriptomic data (Supplemental Fig. S2; Schmid et al., 2003). In addition, fluorescence imaging revealed spatial overlap of LFY, ANT, and, AIL6 protein accumulation in incipient cauline leaf primordia and the first flower primordia (Fig. 2, B–E; Supplemental Fig. S2). The spatiotemporal expression of *ANT*, *AIL6*, and *LFY* is consistent with a possible role of ANT and AIL6 upstream of *LFY* during the meristem identity transition.

With regards to the biphasic transition to flower formation in Arabidopsis, LFY primarily promotes the transition from the prefloral to the floral inflorescence phase and has little or no effect on the vegetative to prefloral inflorescence phase transition. Thus, compared to the wild type, *lfy* mutants display a large increase in the number of cauline leaves and associated secondary inflorescences yet little or no increase in the number of rosette leaves initiated or in the time to bolting (Weigel et al., 1992; Weigel and Nilsson, 1995;

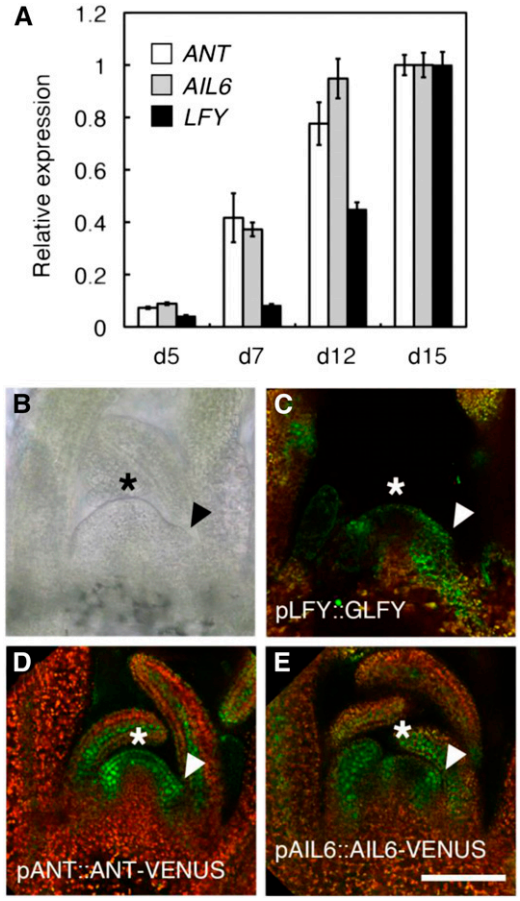

Figure 2. Spatial and temporal accumulation of ANT, AIL6, and LFY. A, Temporal upregulation of *ANT*, *AIL6*, and *LFY* mRNA expression in wild-type plants. The level of gene expression normalized to that of *EIF4* is shown relative to the maximal expression level (in 15-d-old plants) set to 1.0. Shown are mean ± SEM. B, Section of wild-type seedling at the time of the meristem identity transition. C to E, Accumulation of pLFY::GFP-LFY (pLFY::GLFY; C), pANT::ANT-VENUS (D), and pAIL6::AIL6-VENUS (E) proteins in incipient primordia in seedlings at the time of the meristem identity transition. Arrowheads mark the first incipient flower primordium. Asterisks, Inflorescence meristem. Images in B to E are shown at the same magnification. Bar, 50 μm.

Hempel et al., 1997; Ratcliffe et al., 1999; Saddic et al., 2006; Yamaguchi et al., 2009, 2014; Pastore et al., 2011). To test for a role of ANT and AIL6 in regulating *LFY* activity, we therefore next measured the duration of the prefloral inflorescence phase by counting the number of cauline leaves and secondary inflorescences formed in *ant-4* and *ail6-2* single mutants and in wild-type plants (Saddic et al., 2006; Yamaguchi et al., 2009). There was no statistically significant difference between wild type and *ant-4* ($P = 0.68$) or *ail6-2* ($P = 0.72$) single mutants with respect to the time to flower formation (Fig. 3A). This may be due to redundancy between ANT and AIL6, which are known to have overlapping functions in other aspects of reproductive development (Krizek, 2009). To further test this hypothesis, we characterized the timing of the onset of flower formation in *ant-4 ail6-2* double mutants. *ant-4 ail6-2* displayed a significant increase in the number of cauline leaves and secondary inflorescences compared with the wild type ($P < 10^{-4}$). This increase was as strong as that observed in weak *lfy-5* mutants (Fig. 3A). These results suggest that ANT and AIL6 act redundantly in the timing of the formation of the first flower in Arabidopsis.

To test whether ANT and AIL6 act upstream of and in the same pathways as *LFY*, we provided LFY activity from a heterologous promoter in the *ant-4 ail6-2* double mutant and again assessed the timing of the onset of flower formation by counting the number of cauline leaves and secondary inflorescences generated. *ant-4 ail6-2* 35S::LFY plants produced significantly fewer cauline leaves and secondary inflorescences than *ant-4 ail6-2* ($P < 0.001$ and $P < 1.0 \times 10^{-13}$, respectively;

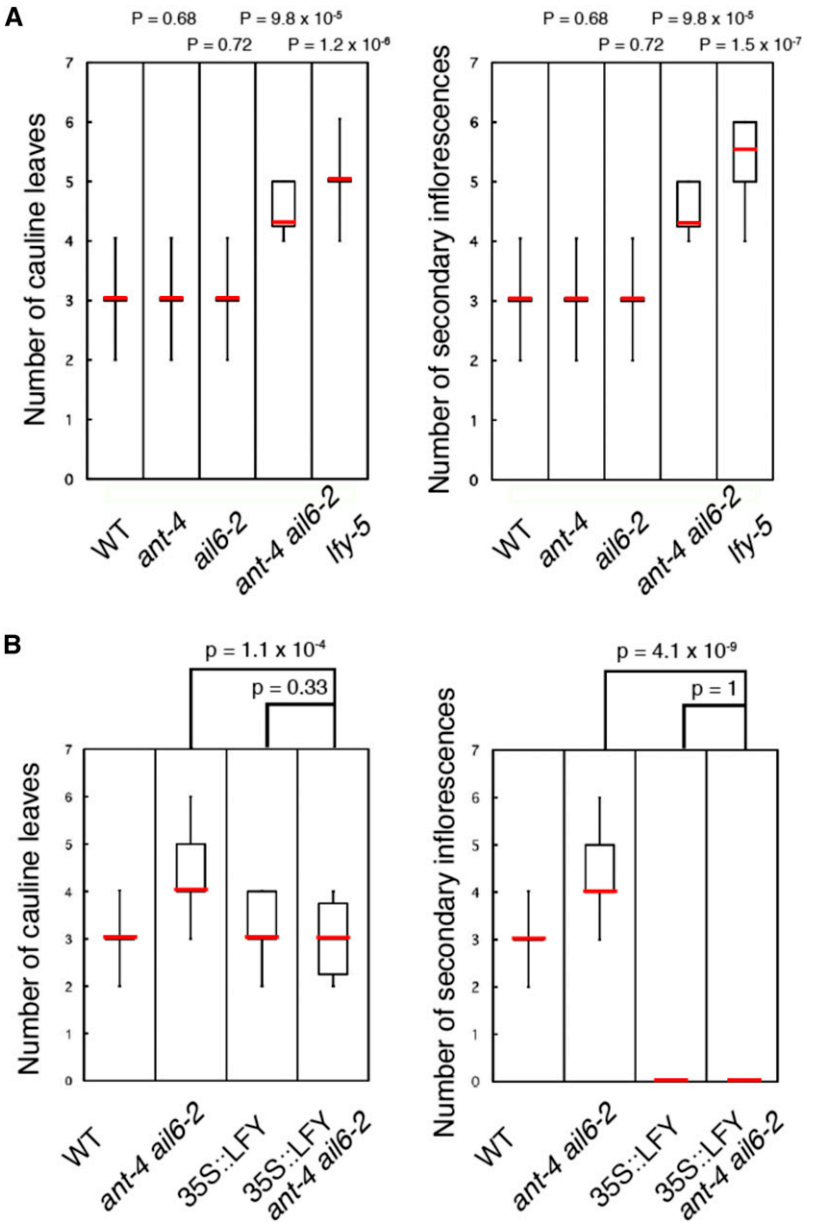

Figure 3. Delayed onset of flower formation in *ant ail6* double mutants and phenotypic rescue of this defect by LFY overexpression. A, Quantification of the number of cauline leaves (left) and secondary inflorescence branches (right) formed. $n \geq 20$ for each genotype tested. *P* values, Two-sided Student's *t* test relative to the wild type. B, Quantification of the number of cauline leaves (left) and secondary inflorescence branches (right) formed in wild type, *ant-4 ail6-2*, 35S::LFY, and *ant-4 ail6-2* 35S::LFY. $n \geq 20$ for each genotype tested. Because the number of secondary inflorescences was not normally distributed, we performed the Kolmogorov-Smirnov test to calculate *P* values. Sample minimum, Lower bar; lower quartile, box; median, red line; upper quartile, box; sample maximum, upper bar.

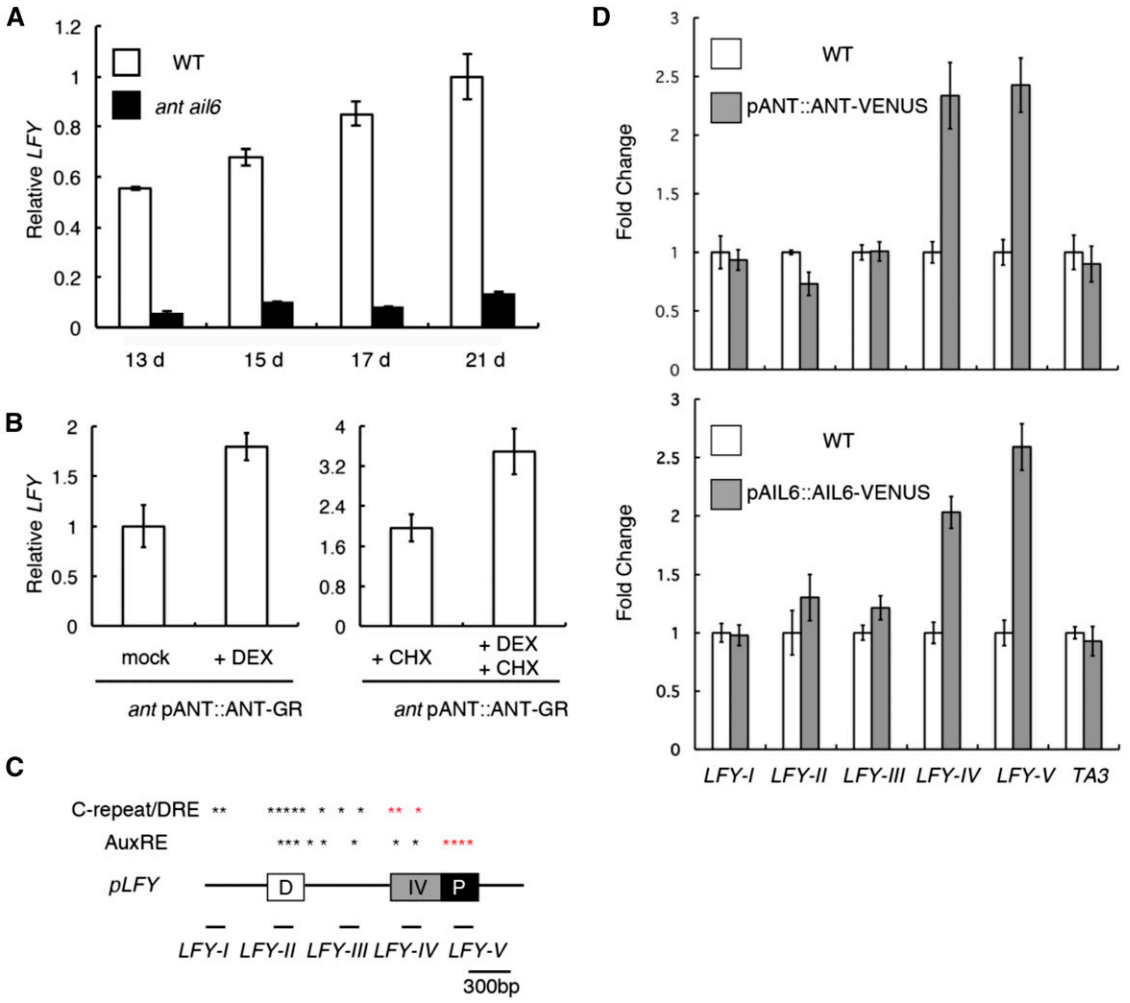

Figure 4. ANT and AIL6 directly induce *LFY* expression. A, Temporal accumulation of *LFY* mRNA in wild-type and *ant-4 ail6-2* double mutant plants. Shown are mean ± SEM. B, *LFY* mRNA levels in *ant* pANT::ANT-GR inflorescences treated with mock or steroid (DEX) solution in the absence (left) or presence (right) of the protein synthesis inhibitor CHX. C, Schematic of the *LFY* promoter. Asterisks show possible cis elements. Top: Potential (black asterisks) and likely ANT/AIL6 bound (red asterisks) C-repeat/DRE core motifs (CCG). Bottom: Potential (black asterisks) and bound (red asterisks) MP consensus motifs (core AuxREs). Regions D (white box) and P (black box) are conserved and functionally important cis regulatory modules of the *LFY* promoter. Region IV (gray box) corresponds to the *LFY-IV* PCR fragment in D. D, Anti-GFP ChIP in pANT::ANT-VENUS (top) and pAIL6::AIL6-VENUS (bottom) relative to wild-type inflorescences. ANT and AIL6 bind to regions IV and V (which is located in the P module in C) in vivo. *TA3*, Negative control locus.

Fig. 3B). The number of cauline leaves in *ant ail6* 35S::LFY did not significantly differ from those observed in 35S::LFY plants ($P = 0.27$; Fig. 3B). Like 35S::LFY plants (Weigel and Nilsson, 1995), *ant-4 ail6-2* 35S:LFY plants formed no secondary inflorescences. Thus, gain-of-LFY function is epistatic to loss of *ANT* and *AIL6* function. The delayed meristem identity transition in *ant-4 ail6-2* double mutants is hence likely attributable to a role for ANT and AIL6 upstream of *LFY*.

ANT and AIL6/PLT3 Directly Induce *LFY* Expression

To test whether ANT and AIL6 regulate *LFY* expression, we examined *LFY* mRNA accumulation in *ant ail6* mutant relative to wild-type plants. In wild type, *LFY* transcripts increased gradually during the meristem identity transition (Fig. 4A). The *ant ail6* mutant showed reduction of *LFY* expression at all time points we tested based on qRT-PCR (Fig. 4A). By contrast, no difference in the expression of a flowering time regulator was observed between wild type and *ant ail6* (Supplemental Fig. S3).

To test whether ANT can directly induce *LFY*, we generated an inducible version of ANT expressed from its own promoter (pANT::ANT-GR) in the *ant-4* background. Activation of the pANT::ANT-GR transgene led to complementation of *ant* defects in petal and stamen growth (Elliott et al., 1996; Klucher et al., 1996), suggesting that the fusion protein is biologically active (Supplemental Fig. S4). Dexamethasone (DEX)

activation of *ant* pANT::ANT-GR in inflorescences led to a 1.7-fold increase in *LFY* expression relative to mock-treated *ant* pANT::ANT-GR (Fig. 4B). To elucidate whether the upregulation of *LFY* upon *ant* pANT::ANT-GR activation required protein synthesis, we examined the effect of *ant* pANT::ANT-GR activation on *LFY* expression in the presence of the protein synthesis inhibitor cycloheximide (CHX). Simultaneous application of CHX and DEX led to increased expression of *LFY* after 3 h (Fig. 4B). Thus, ANT can induce *LFY* in the absence of protein synthesis.

To further test whether ANT and AIL6 directly modulate *LFY* expression, we probed ANT and AIL6 occupancy at the *LFY* locus by chromatin immunoprecipitation (ChIP). Toward this end, we used VENUS-tagged ANT and AIL6 transgenic lines under the control of their own promoters (pANT::ANT-VENUS and pAIL6::AIL6-VENUS; Yamaguchi et al., 2013). By ChIP-qPCR, we detected selective binding of ANT and AIL6 at two of five tested positions at the *LFY* locus, to PCR fragments *LFY-IV* and *LFY-V* (Fig. 4, C and D; Supplemental Fig. S5). Selective ANT occupancy at *LFY-IV* and *LFY-V* regions was

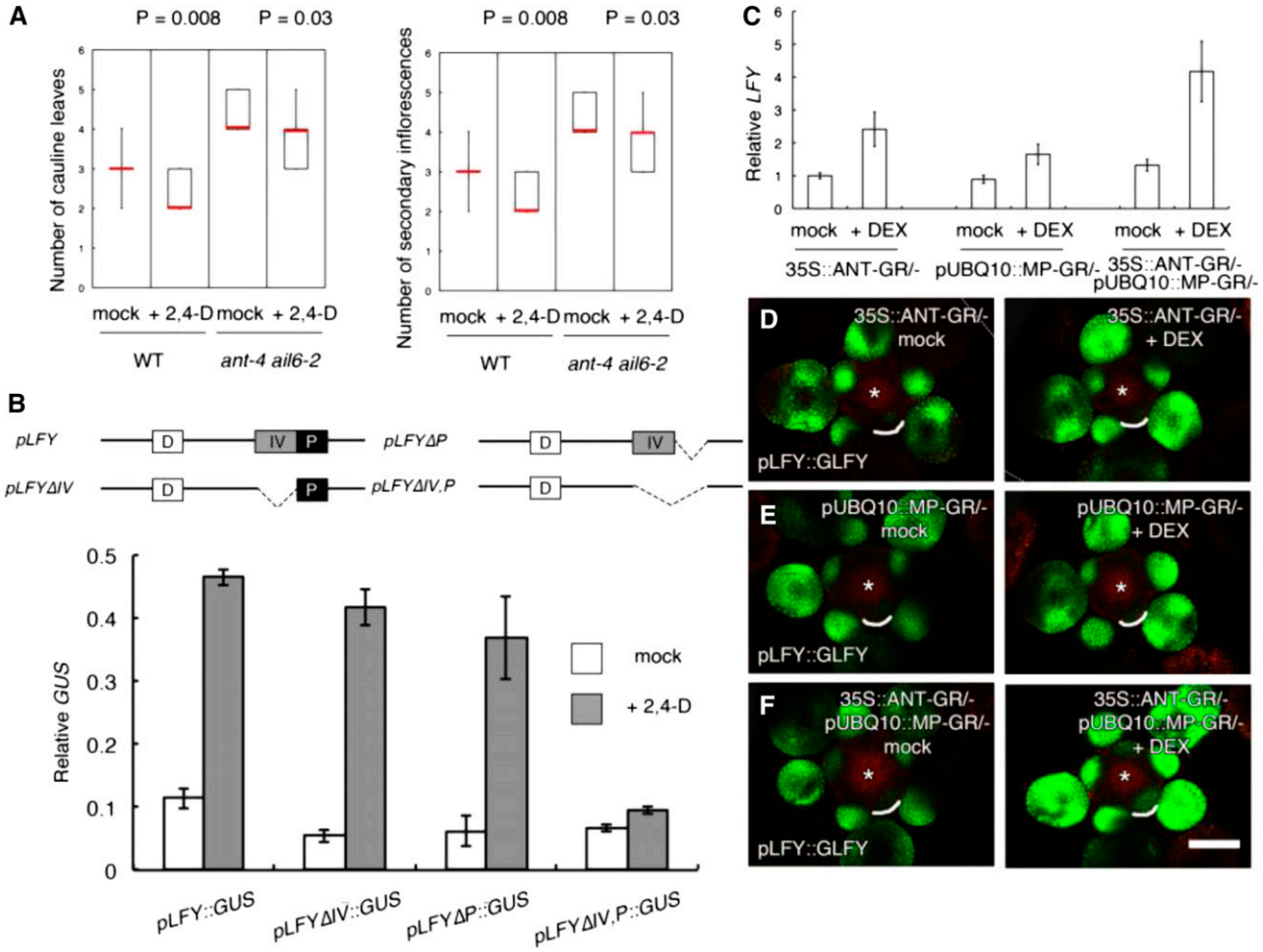

Figure 5. Additive roles for ANT/AIL6 and MP *LFY* induction. A, Quantification of the number of cauline leaves (top) and secondary inflorescence branches (bottom) formed in mock- and 2,4-D-treated (10 μM) wild-type (WT) and *ant-4 ail6-2* plants. $n \geq 12$ for each genotype tested. Sample minimum, Lower bar; lower quartile, box; median, red line; upper quartile, box; sample maximum, upper bar. *P* values, Two-sided Student's *t* test. B, Top: Diagram of *LFY* promoter deletion constructs. Boxes denote critical regions of the *LFY* promoter (see also Fig. 4C). Broken lines, Deletion. Bottom: *GUS* mRNA accumulation determined by qRT-PCR in reporter constructs driven by full-length upstream intergenic region (*pLFY::GUS*), *pLFY::GUS* lacking region IV, (*pLFYΔIV::GUS*), lacking the P region (*pLFYΔP::GUS*), or lacking both the P and the IV region (*pLFYΔIV, P::GUS*). RNA was isolated 3 h after application of mock or 2,4-D (10 μM) solution. Shown is the mean and SEM of *GUS* expression in representative transgenic plants normalized over that of *UBQ10* (*At4g05320*). C, Expression of *LFY* mRNA in mock- and DEX-treated 35S::ANT-GR/-, pUBQ10::MP-GR/-, or 35S::ANT-GR/- pUBQ10::MP-GR/- inflorescences. Shown are mean ± SEM. D to F, Expression of the LFY protein (pLFY::GLFY) in mock- versus DEX-treated 35S::ANT-GR (D), pUBQ10::MP-GR/- (E), or 35S::ANT-GR/- pUBQ10::MP-GR/- (F) inflorescences. Photos for GFP fluorescence (D–F) are from the same experiment, taken using the same confocal microscope setting, and shown at the same magnification. White outline, Flower primordium beginning to grow out; asterisks, inflorescence meristem. Bar, 50 μm.

confirmed using an independent transgenic line and a different antibody (compare Fig. 4D and Supplemental Fig. S6). The *LFY-V* region corresponds to the proximal (P) region of the *LFY* promoter. We will refer to the second fragment bound by ANT and AIL6 as region IV. This region contains three C-repeat core motifs (Fig. 4C). These motifs are bound weakly by ANT in vitro (Nole-Wilson and Krizek, 2000). No strong ANT or AIL6 binding was observed to other regions of the *LFY* promoter (Fig. 4, C and D). We conclude that ANT and AIL6 associate not only with the P region, but also with the adjacent IV region to activate *LFY* expression.

ANT and AIL6 Contribute to the Auxin-Mediated Acceleration of the Switch to Flower Formation in Parallel with MP

Because auxin triggers acceleration of the switch to flower formation in Arabidopsis (Yamaguchi et al., 2013), we next investigated whether ANT and AIL6 contribute to this response. As previously reported (Yamaguchi et al., 2013), the number of cauline leaves and secondary inflorescences formed in the wild type was significantly lower in plants treated with 10 μM 2,4-D than in those treated with mock solution ($P = 0.008$; Fig. 5A). By contrast, the response of *ant-4 ail6-2* plants to the auxin treatment was attenuated (Fig. 5A); the median number of cauline leaves and secondary inflorescences formed was identical in mock- and auxin-treated *ant-4 ail6-2* plants. However, *ant-4 ail6-2* mutant plants still showed some response to auxin ($P = 0.03$ for cauline leaves and secondary inflorescences). The residual auxin responsiveness of *ant ail6* double mutants is likely attributable to MP, which also induces *LFY* in response to auxin (Yamaguchi et al., 2013). We conclude that ANT and AIL6 contribute to the auxin-mediated acceleration of the switch to flower formation in Arabidopsis but are not solely responsible for this phenomenon.

Because ANT and AIL6 bind to both the P and the IV region of *LFY* promoter, we investigated whether deletion of both regions in the context of the full-length *LFY* promoter results in loss of auxin responsiveness. Our findings in Figure 1 above suggest that redundant activities mask the effect of mutation of the MP-bound AuxREs in the P region of *LFY* promoter. In agreement with this interpretation, *pLFYΔP::GUS* was still responsive to 2,4-D (Fig. 5B). We next deleted the IV region of the *LFY* regulatory region, which is bound by ANT and AIL6, but not by MP (Fig. 5B; Yamaguchi et al., 2013). We did not observe a reduction in auxin responsiveness by deleting this region alone (*pLFYΔIV::GUS*; Fig. 5B). However, when we deleted both the P region (which is bound by both MP and ANT/AIL6) and the adjacent IV region (bound only by ANT/AIL6), we observed loss of auxin responsiveness in *pLFYΔIV, P::GUS* (Fig. 5B). An auxin-upregulated gene, *MP* (Lau et al., 2011), and endogenous *LFY* served as treatment controls (Yamaguchi et al., 2013; Supplemental Fig. S7). These data support the hypothesis that not only MP but also both ANT and AIL6 contribute to auxin-mediated *LFY* induction.

We next assessed whether MP and ANT/AIL6 act in parallel pathways. Because the *mp ant ail6* triple mutant does not form flower primordia (Yamaguchi et al., 2013), we instead asked this question by providing both ANT and MP activity conditionally from heterologous promoters. Simultaneous activation of 35S::ANT-GR/- and pUBQ10::MP-GR/- led to much stronger induction of *LFY* on the basis of qRT-PCR than did activation of 35S::ANT-GR/- or UBQ10::MP-GR/- alone (Fig. 5C). This suggests an additive effect of the simultaneous increase in ANT and MP activities on *LFY* mRNA accumulation. We also examined the effect of simultaneous activation of ANT and MP on LFY protein accumulation. Consistent with the qRT-PCR data, we detected a visible increase in LFY protein levels in DEX-treated 35S::ANT-GR/- pUBQ10::MP-GR/- relative to DEX-treated 35S::ANT-GR/- or pUBQ10::MP-GR/- alone (Fig. 5, D–F). The combined data suggest that MP and ANT act in parallel pathways to induce *LFY* expression.

DISCUSSION

The AIL/PLT Transcription Factors ANT and AIL6/PLT3 Directly Induce *LFY* to Promote the Switch to Flower Formation

Molecular genetic studies have identified members of the AIL/PLT family of transcription factors as central regulators of Arabidopsis phyllotaxis, flower primordium outgrowth, flower patterning, and floral organ growth (Elliott et al., 1996; Krizek, 1999, 2009; Mizukami and Fischer, 2000; Prasad et al., 2011; Pinon et al., 2013; Yamaguchi et al., 2013). Here, we show that two members of this family, ANT and AIL6, contribute to the timing of the onset of flower formation by modulating *LFY* expression. The evidence in support of this conclusion is 3-fold. First, *ANT* and *AIL6* mRNA accumulation precedes that of *LFY* and all three proteins are expressed in incipient primordia, where LFY specifies floral fate. Second, *LFY* accumulation is delayed in *ant ail6* double mutants. Third, the delayed transition to flower formation in *ant ail6* double mutants was fully rescued by providing LFY function from a heterologous promoter, suggesting that LFY acts downstream of and in the same pathway as ANT and AIL6. Finally, the induction of *LFY* by ANT is likely direct as it was protein synthesis independent and because ANT and AIL6 were recruited to the *LFY* promoter. We conclude that *ANT* and *AIL6* act redundantly to control *LFY* induction and the timing of flower formation.

ANT and AIL6 both bound to the evolutionarily conserved proximal region (P) of the *LFY* promoter, which is occupied by several other transcription factors in vivo and in vitro, including MP (Blázquez and Weigel, 2000; Gocal et al., 2001; Yamaguchi et al., 2013). ANT and AIL6 also bound to a region of the *LFY* promoter adjacent to the P region, which we called region

IV. Thus far, no other transcription factor has been shown to bind to this region of the *LFY* promoter. Importantly, only deletion of both the IV and the P region led to loss of auxin responsiveness in the context of the full-length *LFY* promoter. These data support the conclusion that ANT and AIL6 contribute to *LFY* induction upon auxin sensing. In addition, they uncover a new region of the *LFY* promoter that contributes to auxin responsiveness. DNA binding properties of ANT have been determined previously (Nole-Wilson and Krizek, 2000). ANT contains two AP2 repeats, and both AP2 repeats are needed to contact DNA. Thus, the ANT binding site is much longer than those recognized by other transcription factors (Franco-Zorrilla et al., 2014). A cis element similar to the in vitro defined ANT consensus-binding motif [5′-gCAC(A/G)N(A/T)TcCC (a/g)ANG(c/t)-3′] is present in the D region of the *LFY* promoter, but not in the P region or the IV region, where we see ANT binding in vivo. ANT can also weakly bind to the C-repeat/DRE elements that show some similarity to the ANT consensus site (Stockinger et al., 1997; Nole-Wilson and Krizek, 2000). We identified three C-repeat/DRE (CCG) core elements in the IV region. These elements may recruit ANT and AIL6 to the *LFY* promoter. No ANT binding motifs were present in the P region. It is currently not understood how ANT or AIL6 are recruited to this region.

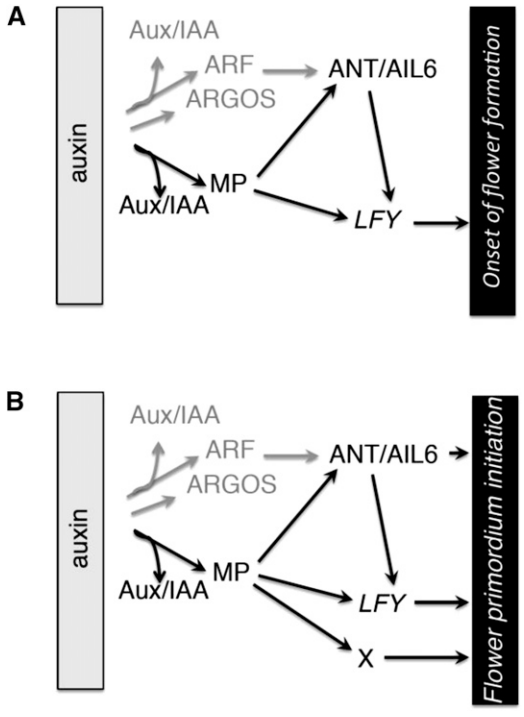

Figure 6. Regulation of the onset of flower formation by auxin. A, Model of the onset of flower formation by auxin. The auxin-activated ARF5/MP transcription factor directly activates *LFY*. Likewise, ANT and AIL6/PLT3 directly induce *LFY* upon auxin sensing to promote the switch to flower formation. ANT/AIL6 and MP act in parallel pathways. This suggests the presence of a MP independent pathway for *ANT/AIL6* induction by auxin. B, Model of flower primordium initiation by auxin. Subsequent to the switch to flower formation, which happens once in the lifecycle of monocarpic plants, both ANT/AIL6 and LFY promote initiation of primordia. See text for additional details.

Two Parallel Pathways for Auxin-Mediated *LFY* Induction

Several pieces of evidence suggest that the AIL/PLT family proteins ANT and AIL6 act together with other regulators to mediate auxin-dependent upregulation of *LFY* during the switch to flower formation. The delay of the switch to flower formation in *ant ail6* double mutants was similar to that of the *lfy-5* hypomorph, but not as strong as that of the *lfy* null mutant. In addition, while *ant ail6* mutants displayed a reduced response to auxin, auxin treatment still accelerated the switch to flower formation in this genetic background. These data suggest the presence of another factor that mediates auxin-dependent *LFY* induction. Some of the remaining activity may be attributable to another AIL/PLT family member that acts together with ANT and AIL6 in this pathway (Aida et al., 2004; Blilou et al., 2005; Krizek, 2011b; Prasad et al., 2011; Hofhuis et al., 2013; Pinon et al., 2013). A second, not mutually exclusive possibility is that ANT/AIL6 induce *LFY* upon auxin sensing at least in part in parallel with MP (Yamaguchi et al., 2013; Fig. 6A). Parallel roles for ANT/AIL6 and MP in this process are supported by the observed additive effects on *LFY* mRNA accumulation of simultaneous activation of MP and ANT. They are further supported by the combined promoter deletion and mutation studies presented here and previously, which implicate both the MP-bound AuxREs (Yamaguchi et al., 2013) and the ANT/AIL6-bound region IV in auxin-dependent *LFY* induction.

Interestingly, ANT and AIL6 are also direct MP targets in inflorescences (Yamaguchi et al., 2013) and act downstream of MP in initiation of flower primordia (Fig. 6B). Data presented here point to parallel roles of MP and ANT/AIL6 in auxin-directed *LFY* induction. There is precedent for this type of transcriptional network, where a transcription factor directly activates another transcription factor that subsequently acts in parallel with the first factor. For example, *APETALA1*, a MADS-box transcription factor and important regulator of floral fate, is a direct LFY target (Parcy et al., 1998; Wagner et al., 1999; William et al., 2004; Winter et al., 2011) and acts in parallel with LFY in the switch to flower formation (Ruiz-García et al., 1997). The role for AP1 in parallel with LFY has been attributed to the presence of a second pathway for *AP1* induction that is independent of LFY (Huala and Sussex, 1992; Abe et al., 2005; Wigge et al., 2005). Likewise, we predict the presence of a MP-independent pathway for *ANT* and *AIL6* induction in response to auxin sensing in inflorescences (Fig. 6 and discussion below).

ANT expression is highly dependent on auxin levels; treatment of plants with a polar auxin transport inhibitor led to a rapid decline in the steady-state levels of *ANT* mRNA (Krizek, 2009). One possible mechanism to account for the MP-independent roles of ANT and AIL6

in *LFY* induction is if auxin can promote ANT and AIL6 accumulation or activity at least in part independently of MP (Fig. 6). Consistent with this scenario is the finding that *ANT* and *AIL6* expression was reduced, but not abolished, in *mp* mutants (Yamaguchi et al., 2013). Possible candidates for transcriptional regulators acting in parallel with MP to induce ANT are other ARF proteins, several of which are strongly expressed in the shoot apex (Vernoux et al., 2011). Indeed, multiple ARF proteins act upstream of *PLT* genes during other stages of development. For example, MP and ARF7/NONPHOTOTROPIC HYPOCOTYL4 act upstream of *PLT1* and *PLT2* during embryogenesis, and ARF7 and ARF19 act upstream of *AIL6/PLT3*, *AIL7/PLT7*, and *AIL5/PLT5* in lateral root development (Aida et al., 2004; Hofhuis et al., 2013). In addition, a candidate upstream regulator of *ANT* that is not an ARF has been described in inflorescences, the ARGOS protein (Hu et al., 2003). The auxin induced *ARGOS* gene encodes a protein of unknown function with several predicted transmembrane domains (Hu et al., 2003) that acts upstream of *ANT* in organ size control. In summary, our data suggest the possibility for two independent pathways that direct transcriptional changes downstream of auxin; this mechanism could act as to prevent premature or ectopic activation of auxin-responsive genes.

We show here that during the developmental phase transition that leads to formation of the first flower, ANT/AIL6 act together with MP to promote *LFY* upregulation in response to auxin (Fig. 6A). After this transition, which happens once in the life or monocarpic plants like Arabidopsis, the shoot apex continuously gives rise to flower primordia (Steeves and Sussex, 1989). ANT/AIL6, LFY, and as yet unidentified additional transcriptional regulators together direct formation of flower primordia (Fig. 6B; Yamaguchi et al., 2013). Because *LFY* accumulation is also modulated in incipient flower primordia by ANT and AIL6 (Supplemental Figs. S8 and S9), we posit that during the initiation of flower primordia, *LFY* is both an ANT/AIL6 target and acts in parallel with ANT/AIL6 (Fig. 6B).

MATERIALS AND METHODS

Plant Materials and Treatment

All plants for phenotypic analysis were grown on soil at 22°C to 23°C in a 16 h light/8 h dark cycle. Seedling plants for expression analysis were grown on Murashige and Skoog plates at 23°C in a 16 h light/8 h dark cycle. Most plants were in the Landsberg *erecta* background except for pLFY::GFP-LFY (pLFY::GLFY) and pUBQ10::MP-GR, which were in the Columbia background. To avoid analysis of mixed genetic backgrounds, we performed F1 experiments to test GLFY expression in 35S::ANT-GR/-, 35S::gAIL6/-, and 35S::ANT-GR/-pUBQ10::MP-GR/-. The following plant lines were previously described: *lfy-5* (Weigel et al., 1992); *ant-4 ail6-2* (Krizek, 2009); pLFY::GLFY (Wu et al., 2003); pANT::ANT-VENUS, pAIL6::AIL6-VENUS, and 35S::ANT-GR (Yamaguchi et al., 2013); and pUBQ10::MP-GR (Donner et al., 2009). For RNA isolation and imaging of GFP experiments, DEX and CHX treatments were performed by spraying 30-d-old plants once with 5 μM DEX and/or 50 μM CHX, respectively. For auxin (2,4-D) treatment in wild type and *ant-4 ail6-2*, to examine the number of cauline leaves and secondary inflorescences formed, 8-d-old to 16-d-old soil-grown plants were treated by spraying them with 10 μM 2,4-D once every three days. To examine the auxin responsiveness of the *LFY* promoter, 10 μM 2,4-D or mock solution was applied to 17-d-old T2 plants by spraying. Samples for mRNA isolation were taken 3 h after spraying. To prepare 10 mM 2,4-D stock solution, 24.3 mg of 2,4-D was dissolved in 10 mL of 95% (v/v) ethanol. Stock solution was 1/1000 diluted with 0.1% (v/v) dimethyl sulfoxide and 0.01% (v/v) Silwet L-77 before spraying. Mock solution was used with 0.1% (v/v) dimethyl sulfoxide, 0.01% (v/v) Silwet L-77, and 0.095% (v/v) ethanol.

Plasmid Construction and Plant Transformation

For construction of ANT::ANT-GR, ANT-GR (Yamaguchi et al., 2013) was subcloned into the *Bam*HI/*Xba*I sites of pCGN1547 containing a 3′ NOS terminator sequence. A 6.2-kb *ANT* promoter fragment was digested out of pBluescript (Krizek, 2009) with *Kpn*I and ligated into ANT-GR/pCGN1547-nos. For construction of 35S::gAIL6, a genomic fragment of *AIL6* corresponding to most of the coding region and 900 bp of 3′ sequence was obtained by digestion of BAC F12B17 with *Kpn*I and *Bam*HI and subcloned into BJ36. The first 141 bp of the *AIL6* coding region were added to this genomic fragment by PCR amplification of the region with AIL6-27 and AIL6-44 and digestion with *Kpn*I. This AIL6 genomic sequence was subcloned into the *Eco*RI site of pART7, which contains the *35S* promoter. 35S::gAIL6 containing the entire coding region of the gene and 740 bp of 3′ sequence was then subcloned into the *Not*I site of pMLBart. Both transgenes were transformed into Landsberg *erecta* by vacuum infiltration (Clough and Bent, 1998). To generate the *LFY* promoter mutation constructs, site-directed mutagenesis was performed as previously described (Yamaguchi et al., 2013). The conserved P element uncovered by phylogenetic shadowing is located −122 bp to −431 bp from the translational start site of *LFY* (Yamaguchi et al., 2013). The P elemental adjacent region IV, which contains the qRT-PCR fragment *LFY-IV*, is positioned −432 bp to −1020 bp from the *LFY* translational start site. To generate the *pLFY* ΔIV, ΔP and Δ IV P constructs, PCR fragments from *LFY* promoter minus the deleted region were incorporated with additional *Spe*I sites into the *Sal*I and *Eco*RI sites of the pENTR3C entry vector and subcloned into the pBGWFS7 binary destination vector. Seeds of transgenic plants were screened on soil by spraying with glufosinate ammonium (BASTA) at 1000-fold dilution (Finale, Bayer) five times from 2 d onwards. GUS staining and qRT-PCR in the presence and absence of auxin was performed in the T1 generation of >25 independent lines. Representative T2 lines were chosen by the same expression pattern in the emerging inflorescence, as well as mature inflorescence, after bolting with T1 lines. These T2 lines assayed for *GUS*, *MP*, and endogenous *LFY* accumulation in the absence and presence of 2,4-D (10 μM). See Supplemental Table S1 for cloning primers used.

Scanning Electron Microscopy

Tissue for scanning electron microscopy was fixed and dehydrated as described previously (Krizek, 1999) and imaged on a FEI Quanta 200 environmental scanning electron microscope.

Confocal Microscopy

Imaging of GFP fluorescence was performed as previously described (Yamaguchi et al., 2013). Inflorescence apices were dissected to remove older flowers prior to observation. A vibratome was used for longitudinal sections to observe primordia at the time of the meristem identity transition. Fifteen-day-old seedlings were imbedded in 5% (v/v) agar, and 50 μm sections were prepared. Tissues were imaged for green and red fluorescence using a Leica confocal microscope (LCS SL) equipped with an argon-krypton ion laser with the appropriate filter sets for visualizing GFP and propidium iodide. Images are maximum projection of z-stacks that include the initiating flower primordia. The same offset and gain settings were used for plants for which signal intensity was directly compared.

qRT-PCR

For Figures 1B, 2A, 4, A and B, and 5B and Supplemental Figures S1, S3, and S7, RNA was extracted from seedling apices containing a few leaf primordia. Older leaves, hypocotyls, and roots were removed by tweezers. For Figure 5C and Supplemental Figures S8 and S9, RNA was extracted from inflorescence apices. Older flowers (stage 12 onward) were removed using tweezers. For GUS qRT-PCR, the 2,4-D responsiveness test was performed with 17-d-old T2 plants. RNA extraction, RNA purification, reverse transcription, and RT-PCR were performed as previously described (Yamaguchi et al., 2013). RT-PCR

experiments were normalized over the ubiquitously expressed *EIF4A* or *UBQ10* genes (*At3g13290* or *At4g05320*, respectively) or At4g12240 (Supplemental Fig. S9). The mean and SEM were determined using at least three technical replicates from one representative experiment. Two or three independent experiments were performed. See Supplemental Table S1 for qRT-PCR primers used.

ChIP

ChIP was performed as previously described (Yamaguchi et al., 2013). A total of 300 mg tissue from inflorescences was used with 10 μL/sample of anti-GFP antibody A6455 (Invitrogen) or 5 μL/sample of anti-HA antibody 12CA5 (Roche). The signal obtained for the genetic control ChIP (anti-GFP or anti-HA ChIP performed on same stage nontransgenic plants) was set to 1.0, and the signal for the experimental ChIP is expressed as fold-increase above the genetic control signal. The mean and SEM were determined using at least three technical replicates from one representative experiment. Two or three independent experiments were performed. See Supplemental Table S1 for ChIP primers used.

Supplemental Data

The following supplemental materials are available.

Supplemental Figure S1. *MP* and *LFY* mRNA accumulation in T2 reporter lines.

Supplemental Figure S2. Expression of *ANT*, *AIL6*, and *LFY* is developmentally regulated.

Supplemental Figure S3. *FLOWERLING LOCUS T* (*FT*) mRNA accumulation in *ant ail6* mutant.

Supplemental Figure S4. *ant* pANT::ANT-GR transgenic plants show complementation of the petal and stamen size defects of *ant* mutants.

Supplemental Figure S5. Analysis of the *LFY* locus by ChIP using GFP antibody.

Supplemental Figure S6. Analysis of ANT-HA binding to the *LFY* locus.

Supplemental Figure S7. *MP* and endogenous *LFY* mRNA accumulation in reporter lines.

Supplemental Figure S8. *LFY* expression in *ANT* and *AIL6* loss- and gain-of-function mutants.

Supplemental Figure S9. Characterization of 35S::gAIL6 transgenic plants.

Supplemental Table S1. Primer sets used in this study.

ACKNOWLEDGMENTS

We thank the Arabidopsis Biological Resource Center for mutant seeds.

Received June 23, 2015; accepted November 3, 2015; published November 4, 2015.

LITERATURE CITED

Abe M, Kobayashi Y, Yamamoto S, Daimon Y, Yamaguchi A, Ikeda Y, Ichinoki H, Notaguchi M, Goto K, Araki T (2005) FD, a bZIP protein mediating signals from the floral pathway integrator FT at the shoot apex. Science **309:** 1052–1056

Aida M, Beis D, Heidstra R, Willemsen V, Blilou I, Galinha C, Nussaume L, Noh YS, Amasino R, Scheres B (2004) The PLETHORA genes mediate patterning of the Arabidopsis root stem cell niche. Cell **119:** 109–120

Araki T (2001) Transition from vegetative to reproductive phase. Curr Opin Plant Biol **4:** 63–68

Bai F, Demason DA (2008) Hormone interactions and regulation of PsPK2: GUS compared with DR5:GUS and PID:GUS in Arabidopsis thaliana. Am J Bot **95:** 133–145

Bäurle I, Dean C (2006) The timing of developmental transitions in plants. Cell **125:** 655–664

Blázquez MA, Ferrándiz C, Madueño F, Parcy F (2006) How floral meristems are built. Plant Mol Biol **60:** 855–870

Blázquez MA, Soowal LN, Lee I, Weigel D (1997) LEAFY expression and flower initiation in Arabidopsis. Development **124:** 3835–3844

Blázquez MA, Weigel D (2000) Integration of floral inductive signals in Arabidopsis. Nature **404:** 889–892

Blilou I, Xu J, Wildwater M, Willemsen V, Paponov I, Friml J, Heidstra R, Aida M, Palme K, Scheres B (2005) The PIN auxin efflux facilitator network controls growth and patterning in Arabidopsis roots. Nature **433:** 39–44

Clough SJ, Bent AF (1998) Floral dip: a simplified method for Agrobacterium-mediated transformation of Arabidopsis thaliana. Plant J **16:** 735–743

Donner TJ, Sherr I, Scarpella E (2009) Regulation of preprocambial cell state acquisition by auxin signaling in Arabidopsis leaves. Development **136:** 3235–3246

Elliott RC, Betzner AS, Huttner E, Oakes MP, Tucker WQ, Gerentes D, Perez P, Smyth DR (1996) AINTEGUMENTA, an APETALA2-like gene of Arabidopsis with pleiotropic roles in ovule development and floral organ growth. Plant Cell **8:** 155–168

Franco-Zorrilla JM, López-Vidriero I, Carrasco JL, Godoy M, Vera P, Solano R (2014) DNA-binding specificities of plant transcription factors and their potential to define target genes. Proc Natl Acad Sci USA **111:** 2367–2372

Gocal GF, Sheldon CC, Gubler F, Moritz T, Bagnall DJ, MacMillan CP, Li SF, Parish RW, Dennis ES, Weigel D, et al (2001) GAMYB-like genes, flowering, and gibberellin signaling in Arabidopsis. Plant Physiol **127:** 1682–1693

Hempel FD, Weigel D, Mandel MA, Ditta G, Zambryski PC, Feldman LJ, Yanofsky MF (1997) Floral determination and expression of floral regulatory genes in Arabidopsis. Development **124:** 3845–3853

Hofhuis H, Laskowski M, Du Y, Prasad K, Grigg S, Pinon V, Scheres B (2013) Phyllotaxis and rhizotaxis in Arabidopsis are modified by three PLETHORA transcription factors. Curr Biol **23:** 956–962

Horstman A, Willemsen V, Boutilier K, Heidstra R (2014) AINTEGUMENTA-LIKE proteins: hubs in a plethora of networks. Trends Plant Sci **19:** 146–157

Hu Y, Xie Q, Chua NH (2003) The Arabidopsis auxin-inducible gene ARGOS controls lateral organ size. Plant Cell **15:** 1951–1961

Huala E, Sussex IM (1992) LEAFY interacts with floral homeotic genes to regulate Arabidopsis floral development. Plant Cell **4:** 901–913

Klucher KM, Chow H, Reiser L, Fischer RL (1996) The AINTEGUMENTA gene of Arabidopsis required for ovule and female gametophyte development is related to the floral homeotic gene APETALA2. Plant Cell **8:** 137–153

Krizek B (2009) AINTEGUMENTA and AINTEGUMENTA-LIKE6 act redundantly to regulate Arabidopsis floral growth and patterning. Plant Physiol **150:** 1916–1929

Krizek BA (1999) Ectopic expression of AINTEGUMENTA in Arabidopsis plants results in increased growth of floral organs. Dev Genet **25:** 224–236

Krizek BA (2011a) Aintegumenta and Aintegumenta-Like6 regulate auxin-mediated flower development in Arabidopsis. BMC Res Notes **4:** 176

Krizek BA (2011b) Auxin regulation of Arabidopsis flower development involves members of the AINTEGUMENTA-LIKE/PLETHORA (AIL/PLT) family. J Exp Bot **62:** 3311–3319

Lau S, Smet ID, Kolb M, Meinhardt, Jurgens G (2011) Auxin triggers a genetic switch. Nat Cell Biol **13:** 611–615

Lee J, Oh M, Park H, Lee I (2008) SOC1 translocated to the nucleus by interaction with AGL24 directly regulates leafy. Plant J **55:** 832–843

Liu C, Chen H, Er HL, Soo HM, Kumar PP, Han JH, Liou YC, Yu H (2008) Direct interaction of AGL24 and SOC1 integrates flowering signals in Arabidopsis. Development **135:** 1481–1491

Mizukami Y, Fischer RL (2000) Plant organ size control: AINTEGUMENTA regulates growth and cell numbers during organogenesis. Proc Natl Acad Sci USA **97:** 942–947

Muller B, Sheen J (2008) Cytokinin auxin interaction in root stem-cell specification during early embryogenesis. Nature **453:** 1094–1097

Nole-Wilson S, Krizek BA (2000) DNA binding properties of the Arabidopsis floral development protein AINTEGUMENTA. Nucleic Acids Res **28:** 4076–4082

Parcy F, Nilsson O, Busch MA, Lee I, Weigel D (1998) A genetic framework for floral patterning. Nature **395:** 561–566

Pastore JJ, Limpuangthip A, Yamaguchi N, Wu MF, Sang Y, Han SK, Malaspina L, Chavdaroff N, Yamaguchi A, Wagner D (2011) LATE MERISTEM IDENTITY2 acts together with LEAFY to activate APETALA1. Development **138:** 3189–3198

Pinon V, Prasad K, Grigg SP, Sanchez-Perez GF, Scheres B (2013) Local auxin biosynthesis regulation by PLETHORA transcription factors controls phyllotaxis in Arabidopsis. Proc Natl Acad Sci USA **110:** 1107–1112

Poethig RS (2003) Phase change and the regulation of developmental timing in plants. Science **301:** 334–336

Prasad K, Grigg SP, Barkoulas M, Yadav RK, Sanchez-Perez GF, Pinon V, Blilou I, Hofhuis H, Dhonukshe P, Galinha C, et al (2011) Arabidopsis PLETHORA transcription factors control phyllotaxis. Curr Biol **21:** 1123–1128

Ratcliffe OJ, Bradley DJ, Coen ES (1999) Separation of shoot and floral identity in Arabidopsis. Development **126:** 1109–1120

Ruiz-García L, Madueño F, Wilkinson M, Haughn G, Salinas J, Martínez-Zapater JM (1997) Different roles of flowering-time genes in the activation of floral initiation genes in Arabidopsis. Plant Cell **9:** 1921–1934

Saddic LA, Huvermann B, Bezhani S, Su Y, Winter CM, Kwon CS, Collum RP, Wagner D (2006) The LEAFY target LMI1 is a meristem identity regulator and acts together with LEAFY to regulate expression of CAULIFLOWER. Development **133:** 1673–1682

Schmid M, Uhlenhaut NH, Godard F, Demar M, Bressan R, Weigel D, Lohmann JU (2003) Dissection of floral induction pathways using global expression analysis. Development **130:** 6001–6012

Steeves TA, Sussex IM (1989) Patterns in Plant Development. Cambridge University Press, Cambridge, UK

Stockinger EJ, Gilmour SJ, Thomashow MF (1997) Arabidopsis thaliana CBF1 encodes an AP2 domain-containing transcriptional activator that binds to the C-repeat/DRE, a cis-acting DNA regulatory element that stimulates transcription in response to low temperature and water deficit. Proc Natl Acad Sci USA **94:** 1035–1040

Vernoux T, Brunoud G, Farcot E, Morin V, Van den Daele H, Legrand J, Oliva M, Das P, Larrieu A, Wells D, et al (2011) The auxin signalling network translates dynamic input into robust patterning at the shoot apex. Mol Syst Biol **7:** 508

Wagner D, Sablowski RWM, Meyerowitz EM (1999) Transcriptional activation of APETALA1 by LEAFY. Science **285:** 582–584

Weigel D, Alvarez J, Smyth DR, Yanofsky MF, Meyerowitz EM (1992) *LEAFY* controls floral meristem identity in *Arabidopsis.* Cell **69:** 843–859

Weigel D, Nilsson O (1995) A developmental switch sufficient for flower initiation in diverse plants. Nature **377:** 495–500

Wigge PA, Kim MC, Jaeger KE, Busch W, Schmid M, Lohmann JU, Weigel D (2005) Integration of spatial and temporal information during floral induction in Arabidopsis. Science **309:** 1056–1059

William DA, Su Y, Smith MR, Lu M, Baldwin DA, Wagner D (2004) Genomic identification of direct target genes of LEAFY. Proc Natl Acad Sci USA **101:** 1775–1780

Winter CM, Austin RS, Blanvillain-Baufumé S, Reback MA, Monniaux M, Wu MF, Sang Y, Yamaguchi A, Yamaguchi N, Parker JE, et al (2011) LEAFY target genes reveal floral regulatory logic, cis motifs, and a link to biotic stimulus response. Dev Cell **20:** 430–443

Wu X, Dinneny JR, Crawford KM, Rhee Y, Citovsky V, Zambryski PC, Weigel D (2003) Modes of intercellular transcription factor movement in the Arabidopsis apex. Development **130:** 3735–3745

Yamaguchi A, Wu MF, Yang L, Wu G, Poethig RS, Wagner D (2009) The microRNA-regulated SBP-Box transcription factor SPL3 is a direct upstream activator of LEAFY, FRUITFULL, and APETALA1. Dev Cell **17:** 268–278

Yamaguchi N, Winter CM, Wu MF, Kanno Y, Yamaguchi A, Seo M, Wagner D (2014) Gibberellin acts positively then negatively to control onset of flower formation in Arabidopsis. Science **344:** 638–641

Yamaguchi N, Wu MF, Winter CM, Berns MC, Nole-Wilson S, Yamaguchi A, Coupland G, Krizek BA, Wagner D (2013) A molecular framework for auxin-mediated initiation of flower primordia. Dev Cell **24:** 271–282

Yoon HS, Baum DA (2004) Transgenic study of parallelism in plant morphological evolution. Proc Natl Acad Sci USA **101:** 6524–6529